




Observations of Short-period Current Sheet Flapping Events in the Earth's Magnetotail

Y. Y. Wei^{1,2}, S. Y. Huang¹, Z. J. Rong^{3,4}, Z. G. Yuan¹, K. Jiang¹, X. H. Deng⁵, M. Zhou⁵, H. S. Fu⁶ , X. D. Yu¹, S. B. Xu¹,
L. H. He¹, and D. Deng¹

¹ School of Electronic Information, Wuhan University, Wuhan, People's Republic of China; shiyonghuang@whu.edu.cn

² Shandong Provincial Key Laboratory of Optical Astronomy and Solar-Terrestrial Environment, Shandong University, Weihai, People's Republic of China

³ Key Laboratory of Earth and Planetary Physics, Institute of Geology and Geophysics, Chinese Academy of Sciences, Beijing, People's Republic of China

⁴ College of Earth and Planetary Sciences, University of Chinese Academy of Sciences, Beijing, People's Republic of China

⁵ Institute of Space Science and Technology, Nanchang University, Nanchang, People's Republic of China

⁶ School of Space and Environment, Beihang University, Beijing, People's Republic of China

Received 2019 February 12; revised 2019 March 11; accepted 2019 March 12; published 2019 March 29

Abstract

The flapping motion of the current sheet, with the period from several minutes to tens of minutes, is one common dynamic phenomenon in the planetary magnetotail. This Letter reports on one current sheet flapping event with the short semi-period of ~ 6 s on 2017 July 17 in the Earth's magnetotail for the first time using the Magnetospheric Multiscale (MMS) mission. This short time period flapping event consists of five consecutive crossings of the current sheet. Based on a multipoint analysis of the MMS, it is found that the first four crossings propagated duskward and belong to kink-like flapping, and the fifth crossing belongs to steady flapping. The current sheet flapping was embedded in the diffusion region of magnetic reconnection, which was identified by the well-organized Hall electromagnetic field. The period of current sheet flapping was modulated by the reconnection electric field and perpendicular plasma flow, indicating that this flapping motion may be triggered by the periodical unsteady magnetic reconnection.

Key words: instabilities – magnetic reconnection – planets and satellites: general – planets and satellites: magnetic fields – planets and satellites: terrestrial planets

1. Introduction

The flapping motion of the planetary magnetotail is the up and down oscillation of the tail current sheet. The current sheet flapping is widely observed by different spacecraft missions, which can propagate as kink-like waves toward both tail flanks with a velocity of tens of km s^{-1} (e.g., Zhang et al. 2002, 2005; Sergeev et al. 2003, 2004; Runov et al. 2005; Rong et al. 2015a). The period of the flapping can vary from approximately one minute to tens of minutes, and the wavelength generally exceeds $1 R_E$ (the Earth's radius; Rong et al. 2018; Wang et al. 2019). The multipoint satellite measurements showed that the flapping waveform was undulating and that the sequence of oscillations had alternated inclinations of the current sheet (Petrukovich et al. 2006, 2008). The inclinations of the flapping current sheet can be nearly vertical to the equatorial plane, which may be caused by the slippage of the magnetic flux tubes in the flapping plasma sheet (Petrukovich et al. 2006; Shen et al. 2008). At the center of the flapping current sheet, the current density J and its J_z component reach the maximum or have enhancements (i.e., J_z will change its signs between the two flappings), and meanwhile the curvature of the magnetic field lines reaches the minimum (Petrukovich et al. 2008; Rong et al. 2010). The current sheet flapping can be divided into two types according to its propagation: one is kink-like flapping that propagates dawnward or duskward as waves; the other one is steady flapping that flaps as stationary waves (only up and down oscillations in the south–north

direction and without propagation). The kink-like flapping at a higher frequency travels faster, and has a shorter wavelength and a smaller amplitude (Rong et al. 2018). In addition to the kink-like flapping types, Rong et al. (2015b) found that the tail current sheet sometimes just flaps up and down but does not propagate as waves; they refer to this kind of flapping phenomenon as steady flapping. According to the statistical survey, Gao et al. (2018) proposed that the up and down motion of steady flapping tends to occur around the midnight region, which can induce kink-like flapping waves and propagate toward both flanks.

Several mechanisms have been proposed to explain the generation of the current sheet flapping. It was argued that the external disturbance pulses could induce the current sheet flapping as a kink-like wave mode (e.g., Daughton 1999). For example, the pressure pulse associated with a substorm can trigger the kink-like flappings or kink waves (Fruit et al. 2002, 2004). In the kinetic models, kink waves can be induced by the drift of the Kelvin–Helmholtz instability, and this model predicts wave propagation from dawn to dusk at a speed of tens of km s^{-1} (Lapenta & Brackbill 1997; Karimabadi et al. 2003). Although the propagation velocity is reasonable, these mechanisms cannot account for the observed direction of flapping wave propagation from the center of the tail to the two sides (Gao et al. 2018). Recently, it was suggested that the current sheet flapping motion can be generated by the hemisphere-asymmetric nonadiabatic ions (Wei et al. 2015).

In this Letter, using the multipoint analysis of the Magnetospheric Multiscale (MMS) mission, we report a short-period current sheet flapping (the quasi-semi-period is about 6 s) for the first time in the terrestrial magnetotail which may be generated by the unsteady magnetic reconnection.



Original content from this work may be used under the terms of the [Creative Commons Attribution 3.0 licence](https://creativecommons.org/licenses/by/3.0/). Any further distribution of this work must maintain attribution to the author(s) and the title of the work, journal citation and DOI.

2. Observations

We use the magnetic field data from the fluxgate magnetometer (Russell et al. 2016), the electric field data recorded by the electric field double probe (Ergun et al. 2016; Lindqvist et al. 2016), and the plasma data measured by the fast plasma instrument (Pollock et al. 2016) to investigate this short-period current sheet flapping event. Geocentric solar magnetospheric (GSM) coordinates are used in this study unless otherwise specified.

2.1. A Short-period Current Flapping Event in the Terrestrial Magnetotail

The location of the flapping event occurred at $[-17.98, 7.26, 0.65] R_E$. Four spacecraft formed a tetrahedron in space with a separation of ~ 25 km. Due to the identical observations of the four spacecraft, we only present the observations from MMS1 here.

Figure 1 displays the observations of the current sheet flapping in the magnetotail. There are five consecutive crossings of the current sheet with a semi-period of about 6 s as marked by the vertical dashed lines. The Z component of the current J_z is positive at the first and third crossing and then becomes negative at the second and fourth crossing, and slight positive at the fifth crossing. In other words, J_z changes its sign for the neighboring crossings (Figure 1(b)). The radius of curvature (hundreds of kilometers; Figure 1(c)) and the modulus of the gradient of the magnetic field strength (∇B) reach a minimum (Figure 1(d)) at the center of the current sheet. These observations are consistent with the features of the current sheet flapping (Shen et al. 2008), and also similar to previous reports on the flapping characteristics of the terrestrial magnetotail current sheet (e.g., Sergeev et al. 2004; Rong et al. 2010).

According to the diagnosis technique proposed by Shen et al. (2008), ∇B will change its direction during the kink-like flapping of the current sheet. When the flapping propagates toward the dawn side (dusk side), ∇B measured by the four spacecraft will first point dawnward (duskward) with its azimuthal angle $\phi_{\nabla B}$ near to 270° (90°), and then duskward (dawnward) with its azimuthal angle $\phi_{\nabla B}$ near to 90° (270° ; Rong et al. 2010). Thus, we use the azimuthal angle $\phi_{\nabla B}$ obtained by defining the spherical coordinate vector direction ($0^\circ \leq \theta \leq 90^\circ$, $0^\circ \leq \phi \leq 360^\circ$) in the framework of the GSM coordinates (Shen et al. 2008) to determine the propagation of the flapping mode. Figure 1(e) shows the directional angle ($\theta_{\nabla B}$, $\phi_{\nabla B}$) of the gradient of the magnetic field strength. It can be seen that the $\phi_{\nabla B}$ always changes from 90° to 270° for the first four crossings of the current sheet, implying that the first four flappings are the kink-like waves propagating duskward (Rong et al. 2010). As for the fifth flapping, the $\phi_{\nabla B}$ has rapid fluctuations and cannot be used to identify its type. However, the result from a timing analysis shows that the fifth flapping only propagates in the southern direction (shown in Table 1), implying that this flapping oscillates up and down in the south–north direction and can be categorized as a steady type (Shen et al. 2008).

Table 1 shows the normal vectors of the current sheets obtained by a minimum variable analysis (MVA) method and a timing analysis method for each flapping. The calculated normals of the current sheet by a timing analysis demonstrate that the flapping motion should propagate duskward for the first

four crossings and basically flaps along the z-direction for the fifth crossing, which are both consistent with the previous results from the analysis of ∇B in Figure 1(d). The propagation speed of the current sheet increases from 418.74 km h^{-1} to 513.09 km s^{-1} , then gradually decreases to 76.63 km s^{-1} . The angular deviation $\Delta\alpha$ between the normal vector obtained by the MVA analysis and the one determined by the timing analysis are relatively small for the first, second, fourth, and fifth flapping, while the $\Delta\alpha$ is large for the third flapping. Such disagreements between two normal directions may be induced by the fluctuation of B_z near the third flapping (Zhang et al. 2005). The normal vector obtained by the MVA are quasi-parallel to the z-axis for the first, fourth, and fifth flapping and quasi-perpendicular to the z-axis for the second and third flapping, implying that the current sheets are quasi-horizontal during the first, fourth, and fifth flapping, and quasi-vertical to the equatorial plane during the second and third flapping. However, the flapping type can no longer be identified by the MVA method relying on a one-point analysis when the current sheet is quasi-horizontal and quasi-vertical (Rong et al. 2015b).

In order to illustrate the flapping sequence more clearly, the cartoon diagrams were drawn to describe the wavy shape of the flapping event in Figure 1(f).

Therefore, one can conclude that the MMS observed one short-period current sheet flapping event in the terrestrial magnetotail.

2.2. Current Sheet Flapping are Accompanied by Magnetic Reconnection

Figure 2 shows the overview of the observations of magnetic reconnection in the magnetotail from 7:48:30 UT to 7:50:20 UT. Typical plasma sheet ion spectrogram (Figure 2(a)), density (Figure 2(e)), temperature (Figure 2(f)), and plasma β (> 1 ; Figure 2(g)) are detected by the MMS during this time interval (Cao et al. 2006). There is a plasma flow reversal (Figure 2(d)) from tailward ($V_x < 0$) to earthward ($V_x > 0$) accompanied by the variation of B_z from negative to positive (Figure 2(b)), indicating that one tailward retreating x-line of magnetic reconnection possibly passed through the MMS spacecraft (Huang et al. 2010, 2012; Zhou et al. 2014, 2017; Fu et al. 2016). In the tailward flow (07:48:30–07:49:40 UT), B_y has an opposite direction compared to B_x , i.e., positive B_y versus negative B_x , and negative B_y versus positive B_x ; while in the earthward flow (07:49:40–07:50:05 UT), B_y has same direction as B_x . The electric field component E_z (Figure 2(c)) is positive in the southern hemisphere ($B_x < 0$) and negative in the northern hemisphere ($B_x > 0$). These features of B_y and E_z are in accordance to the quadrupolar structure of the Hall magnetic field and bipolar Hall electric field pointing to the center of the current sheet in the magnetic reconnection diffusion region (Eastwood et al. 2010; Huang et al. 2014, 2016, 2018; Fu et al. 2017). Therefore, the current sheet flapping was embedded in the reconnection diffusion region.

To further investigate the relationship between the current sheet flapping and magnetic reconnection, we present magnetic field and electric field and the ion velocity perpendicular to the magnetic field within the time interval of the flapping event in Figure 3. It is clearly seen that the Hall magnetic field (B_y in Figure 3(a)) and Hall electric field (E_z in Figure 3(b)) have the opposite trend of B_x during the flapping. The values of reconnection electric field E_y and the variations of ion flow velocity indicate the changing of reconnection rate

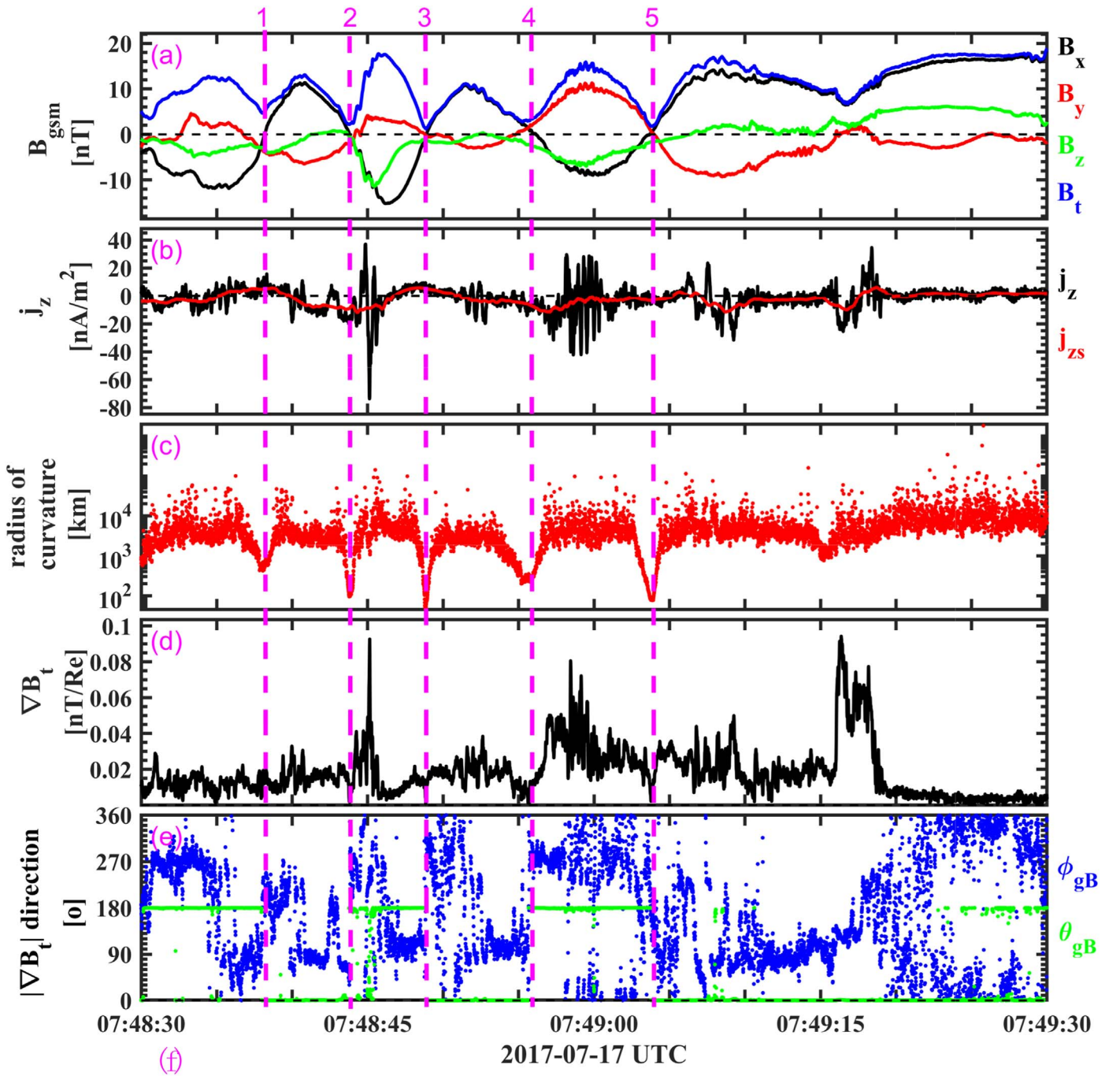


Figure 1. Flapping of the current sheet observed by MMS1 on 2017 July 17 between 07:48:30 UT and 07:49:30 UT. (a) The magnetic field in GSM; (b) the Z component of the current J_z , where the red line represents the smoothed J_z ; (c) the radius of curvature R_c ; (d) the value of the gradient of the magnetic field strength; (e) the directional angle (θ_{gB} , ϕ_{gB}) of the gradient of the magnetic field strength; and (f) a cartoon illustrating the flapping of a current sheet (the former describes the three-dimensional picture of the flapping current sheet, while the latter describes its two-dimensional one).

(Fu et al. 2013a, 2013b, 2019). Especially, the reconnection electric field E_y and the amplitude of perpendicular velocity and X component of ion flow have the same periodic oscillations as

the magnetic field B_x , implying that the current sheet flapping may be modulated by the unsteady magnetic reconnection with the semi-period of ~ 6 s.

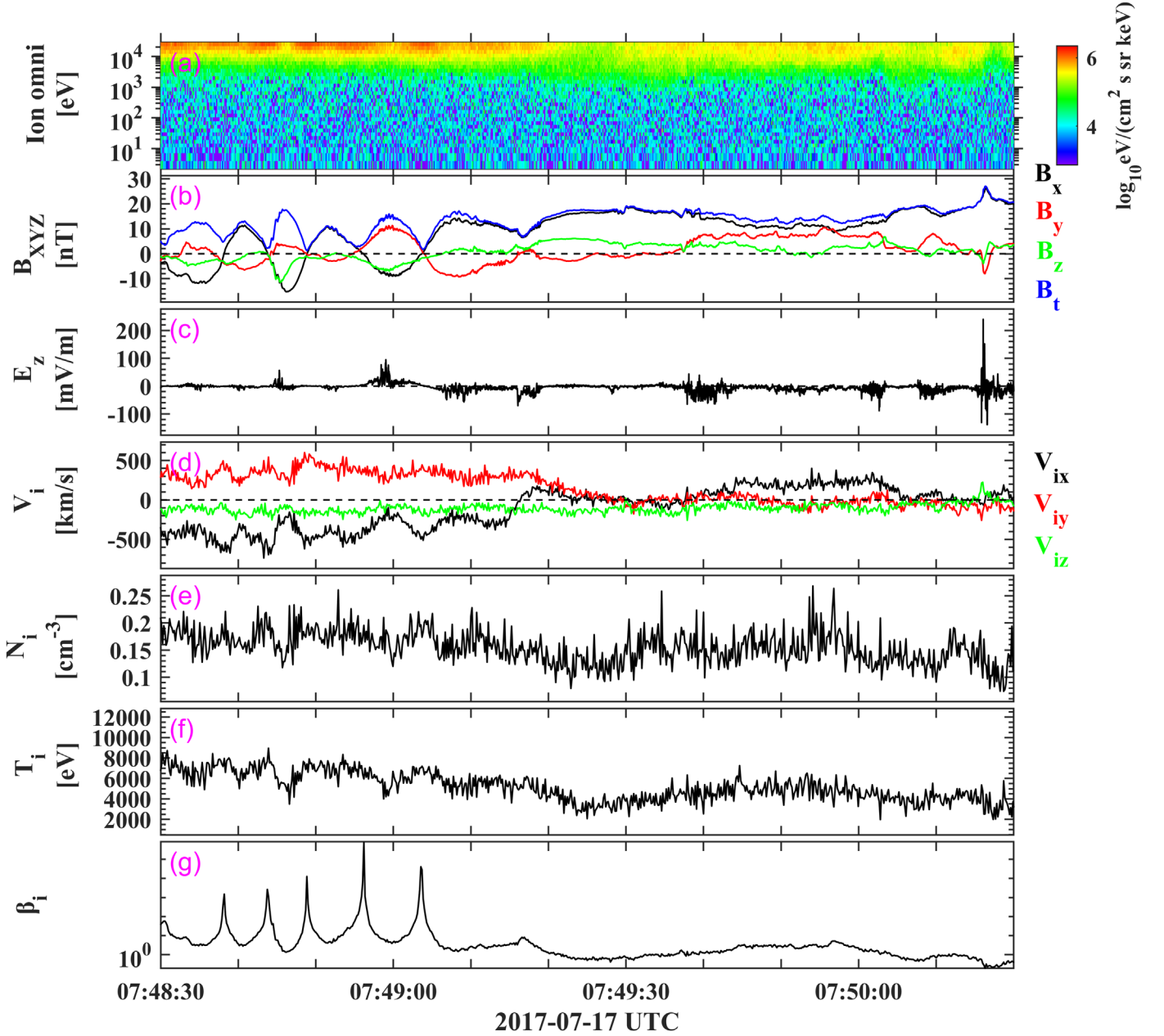


Figure 2. Observations of the magnetic reconnection diffusion region associated with the current sheet flapping. (a) The omnidirectional energy of ions; (b) the magnetic field in GSM; (c) the Hall electric field E_z ; (d) three components of the proton flow velocity; (e) the ion density; (f) ion temperature; and (g) plasma β_i .

Table 1
Minimum Variable Analysis and Timing Analysis for the Current Sheet Crossings on 2017 July 17

Crossing	$\Delta t(s)^a$	Timing Normal ^b	MVA Normal ^c	$\Delta\alpha^d$	λ_2/λ_3^e	V (km s ⁻¹) ^f
#1	3	-0.01 0.33-0.95	0.0018 0.41-0.91	5.44	7.93	418.74
#2	5	0.06 0.88 0.46	0.37 0.93 0.10	27.72	10.99	513.09
#3	5	-0.05 0.30-0.95	0.16 0.98 0.11	79.14	58.80	342.58
#4	9	-0.04 0.48 0.87	0.13 0.56 0.82	10.85	11.35	146.14
#5	4	0.06-0.01-0.998	-0.30-0.10 0.95	164.36	7.10	76.63

Notes.

^a The length of the used time interval for the minimum variable analysis (MVA), centered at the current sheet center.

^b The normals yielded by a timing analysis in the GSM coordinates.

^c The MVA normals of MMS1 in the GSM coordinates.

^d The angular deviation of the MVA normal from the timing normal.

^e The ratios between the intermediate and the minimum eigenvalues.

^f The average speed during the half period by the timing analysis.

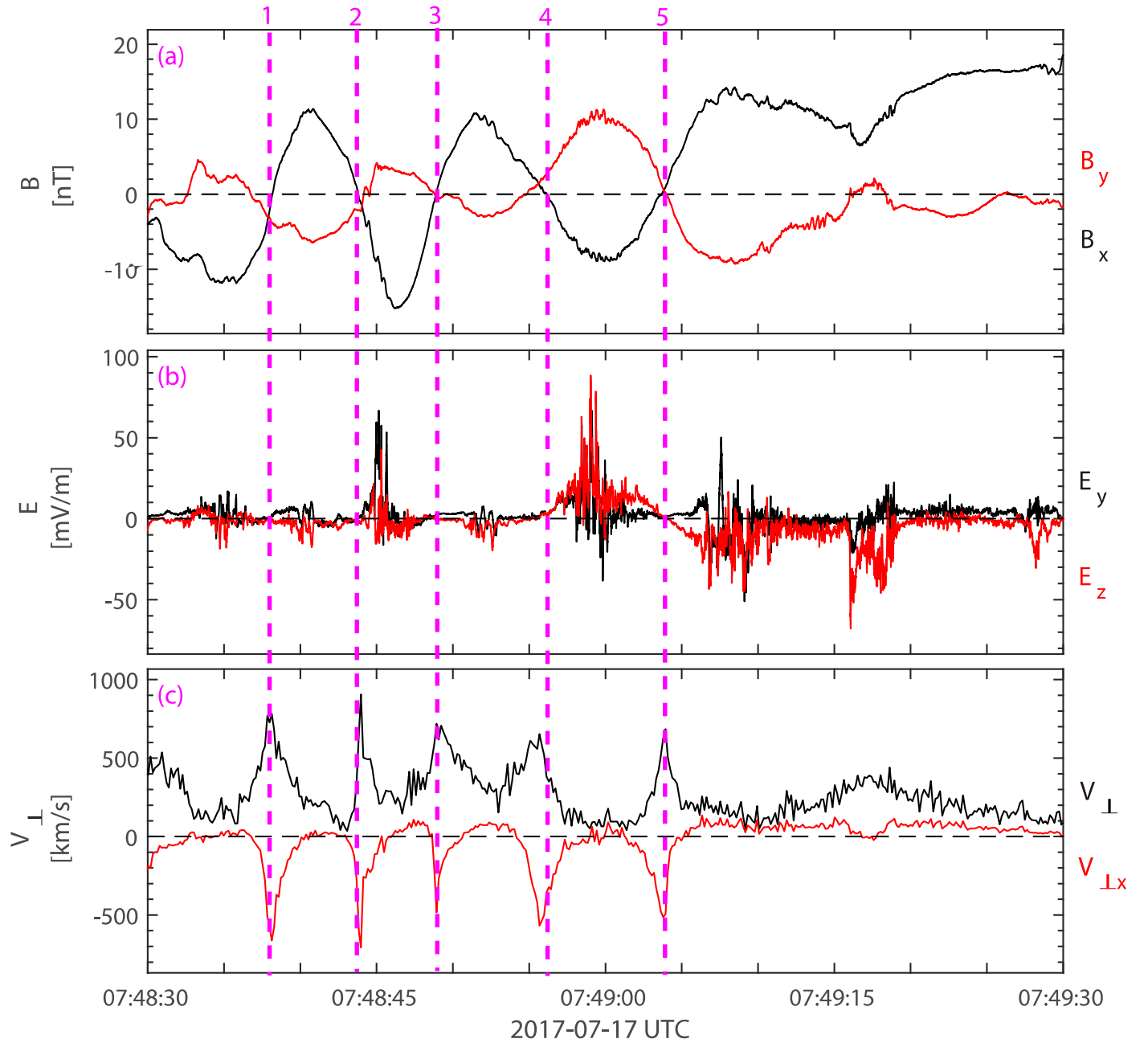


Figure 3. (a) Two components of the magnetic field, B_x and B_y ; (b) the Hall electric field E_z and reconnection electric field E_y ; and (c) the perpendicular velocity V_{\perp} and its X component ($V_{\perp x}$) of perpendicular velocity.

3. Discussion

There are two types of flapping of the current sheet: one is a kinking propagation and the other is steady flapping. Gao et al. (2018) have proposed that the current sheet flapping belongs to a steady type in the midnight sector, and the kink-like flapping propagates at the dusk side and dawn side. Our observations show that the first four short-period flappings are the kink-like flapping propagating duskward in the dusk side of the magnetotail and the last one is the steady flapping, which supports the work of Gao et al. (2018).

The comparisons of the semi-period of the flapping between previous works and present study are shown in Table 2. It can be seen that the flapping in this work has the shortest semi-period. This short-period current sheet flapping in our event has the highest frequency, the highest flapping speed, and the

thinnest thickness, which is consistent with the predictions of Rong et al. (2018). The speed of the flapping with the semi-period of 10 minutes is generally about $10\text{--}20\text{ km s}^{-1}$, while the flapping speed can reach up to 500 km s^{-1} for the flapping with the semi-period of 6 s in our event. This indicates that such short-period flappings can cause the energy to dissipate quickly to both flanks in the magnetotail.

There are various generation mechanisms of the current sheet flapping that can be externally or internally driven. Wei et al. (2015) proposed that the asymmetric motions of nonthermal ions can cause the long-period (up to 5 minutes) current sheet flapping. As for our event, however, the semi-period of the current sheet flapping is only $\sim 6\text{ s}$ (much shorter than that reported by Wei et al. 2015), and there is not any asymmetric motion of the nonthermal ions during the crossings

Table 2
Comparisons of the Current Sheet Flapping Studies

Study	Semi-period	Flap Speed	Half-thickness	Spacecraft
Zhang et al. (2002)	10 minutes	20 km s ⁻¹	^a	Cluster
Sergeev et al. (2003)	1.5 minutes	100 km s ⁻¹	0.36 R _E	Cluster
Sergeev et al. (2004)	6 minutes	20 ~ 80 km s ⁻¹ ,	0.78 R _E	Cluster
Runov et al. (2005)	100 s	30 ~ 70 km s ⁻¹	0.31 ~ 0.47 R _E	Cluster
Zhang et al. (2005)	10 minutes	20 km s ⁻¹	/	Double Star/Cluster
Laitinen et al. (2007)	45 ~ 60 s	60 ~ 170 km s ⁻¹	/	Cluster
Shen et al. (2008)	7 minutes	27 km s ⁻¹	0.14 ~ 0.36 R _E	Cluster
Wei et al. (2015)	5 minutes	/	/	Cluster
Rong et al. (2015b)	1–3 minutes	/	/	Cluster
Gao et al. (2018)	2.5 ~ 7.5 minutes	30 ~ 110 km s ⁻¹	0.31 ~ 0.47 R _E	Cluster
Rong et al. (2018)	5 minutes	30 km s ⁻¹	0.83 R _E	Cluster
	11 minutes	21 km s ⁻¹	0.57 R _E	Cluster
Wang et al. (2019)	4 minutes	60 km s ⁻¹	/	MMS
This Study	6 s	76 ~ 513 km s ⁻¹	0.042R _E	MMS

Note.

^a No data in this work.

of current sheet in our event. Thus, we can rule out the possibility that the short-period flapping was excited by the nonthermal ions. The changes in the direction of the solar wind can drive the flapping of the current sheet (Wang et al. 2019). We examined the solar wind condition before and after the time interval of interest of the observed flapping, and found that the plasma velocity and magnetic field are quiet and did not periodically fluctuate (not shown here). Therefore, the short-period flapping was unlikely caused by the solar wind variations. Laitinen et al. (2007) reported that the current sheet oscillations were observed both before reconnection and during it, and the Hall magnetic field is conforming to the kinks. In our event, the current sheet oscillations are in the reconnection diffusion region with the Hall electromagnetic field structures. The current sheet flapping has the same period of the reconnection electric field and perpendicular plasma flow, suggesting that the observed short-period current sheet flapping may be a consequence of the periodical unsteady reconnection (Sergeev et al. 2006; Fu et al. 2013a, 2013b).

4. Conclusions

In this Letter, we report a short semi-period (down to 6 s) current sheet flapping detected in the terrestrial magnetotail for the first time. The current sheet oscillations result in five consecutive crossings by the MMS spacecraft. The z component of the current J_z reaches maximum at the center of the current sheet (where $B_x \sim 0$), and while the curvature radius and the modulus of the gradient of the magnetic field strength are at their minimum at the center of the current sheet. These observations belong to the features of the flapping of the current sheet. Using of the ∇B azimuth angle to identify the flapping type, we find that the first four crossings are induced by kink-like flapping, while the last one is caused by steady flapping. Based on the results from the timing analysis, we deduce that the current sheets are quasi-horizontal during the first, fourth, and fifth flappings, and quasi-vertical to the equatorial plane during the second and third flappings. In addition, this current sheet flapping is accompanied by the occurrence of magnetic reconnection. The period of the flapping is modulated by the reconnection electric field and perpendicular plasma flow. In this sense, we suggest that the current sheet flapping could be induced by periodical unsteady

magnetic reconnection. Further study is needed to determine the exact relationship between the current sheet flapping and magnetic reconnection.

We thank the entire MMS team and instrument leads for data access and support. This work was supported by the National Natural Science Foundation of China (41674161, 41874191). S.Y.H. acknowledges the project supported by the Specialized Research Fund for Shandong Provincial Key Laboratory and the support by the Young Elite Scientists Sponsorship Program by CAST (2017QNRC001). MMS Data is publicly available from the MMS Science Data Center at <http://lasp.colorado.edu/mms/sdc/>.

ORCID iDs

H. S. Fu  <https://orcid.org/0000-0002-4701-7219>

References

- Cao, J. B., Ma, Y. D., Parks, G., et al. 2006, *JGRA*, **111**, A04206
 Daughton, W. 1999, *PhPl*, **6**, 1329
 Eastwood, J. P., Phan, T. D., Øieroset, M., & Shay, M. A. 2010, *JGRA*, **115**, A08215
 Ergun, R. E., Tucker, S., Westfall, J., et al. 2016, *SSRv*, **199**, 167
 Fruit, G., Louarn, P., Budnik, E., et al. 2004, *JGRA*, **109**, A03217
 Fruit, G., Louarn, P., Tur, A., & Le Queau, D. 2002, *JGRA*, **107**, 1411
 Fu, H. S., Cao, J. B., Khotyaintsev, Y. V., et al. 2013b, *GeoRL*, **40**, 6023
 Fu, H. S., Cao, J. B., Vaivads, A., et al. 2016, *JGRA*, **121**, 1263
 Fu, H. S., Khotyaintsev, Y. V., Vaivads, A., Retinò, A., & André, M. 2013a, *NatPh*, **9**, 426
 Fu, H. S., Vaivads, A., Khotyaintsev, Y. V., et al. 2017, *GeoRL*, **44**, 37
 Fu, H. S., Xu, Y., Vaivads, A., & Khotyaintsev, Y. V. 2019, *ApJL*, **870**, L22
 Gao, J. W., Rong, Z. J., Cai, Y. H., et al. 2018, *JGRA*, **123**, 7413
 Huang, S. Y., Fu, H. S., Yuan, Z. G., et al. 2016, *JGRA*, **121**, 6639
 Huang, S. Y., Jiang, K., Yuan, Z. G., et al. 2018, *ApJ*, **862**, 144
 Huang, S. Y., Pang, Y., YUan, Z., et al. 2014, *ChSbu*, **59**, 4797
 Huang, S. Y., Vaivads, A., Khotyaintsev, Y. V., et al. 2012, *GeoRL*, **39**, L11103
 Huang, S. Y., Zhou, M., Sahraoui, F., et al. 2010, *JGRA*, **115**, A12211
 Karimabadi, H., Daughton, W., Pritchett, P. L., & Krauss-Varban, D. 2003, *JGRA*, **108**, 1400
 Laitinen, T., Nakamura, V. R., Runov, A., Rème, H., & Lucek, E. A. 2007, *AnGeo*, **25**, 1025
 Lapenta, G., & Brackbill, J. U. 1997, *JGRA*, **102**, 27099
 Lindqvist, P.-A., Olsson, G., Torbert, R. B., et al. 2016, *SSRv*, **199**, 137
 Petrukovich, A., Baumjohann, A. W., Nakamura, R., & Runov, A. 2008, *AnGeo*, **26**, 3669

- Petrukovich, A. A., Zhang, T. L., Baumjohann, W., et al. 2006, *AnGeo*, **24**, 1695
- Pollock, C., Moore, T., Jacques, A., et al. 2016, *SSRv*, **199**, 331
- Rong, Z., Barabash, J. S., Stenberg, G., et al. 2015b, *JGRA*, **120**, 3462
- Rong, Z. J., Barabash, S., Stenberg, G., et al. 2015a, *JGRA*, **120**, 5593
- Rong, Z. J., Cai, Y. H., Gao, J. W., et al. 2018, *JGRA*, **123**, 5571
- Rong, Z. J., Shen, C., Petrukovich, A. A., Wan, W. X., & Liu, Z. X. 2010, *P&SS*, **58**, 1215
- Runov, A., Sergeev, V. A., Baumjohann, W., et al. 2005, *AnGeo*, **23**, 1391
- Russell, C. T., Anderson, B. J., Baumjohann, W., et al. 2016, *SSRv*, **199**, 189
- Sergeev, V., Runov, A., Baumjohann, W., et al. 2003, *GeoRL*, **30**, 1327
- Sergeev, V. A., Runov, W., Baumjohann, R., et al. 2004, *GeoRL*, **31**, L05807
- Sergeev, V. A., Sormakov, D. A., Apatenkov, S. V., et al. 2006, *AnG*, **24**, 2015
- Shen, C., Rong, Z. J., Li, X., et al. 2008, *AnGeo*, **26**, 3525
- Wang, G. Q., Zhang, T. L., Wu, M. Y., et al. 2019, *GeoRL*, **46**, 64
- Wei, X. H., Cai, C. L., Cao, J. B., et al. 2015, *GeoRL*, **42**, 4731
- Zhang, T. L., Baumjohann, W., Nakamura, R., et al. 2005, *AdSpR*, **36**, 1940
- Zhang, T. L., Baumjohann, W., Nakamura, R., Balogh, A., & Glassmeier, K.-H. 2002, *GeoRL*, **299**, 1899
- Zhou, M., Ashour-Abdalla, M., Deng, X., et al. 2017, *JGRA*, **122**, 9513
- Zhou, M., Deng, X., Tang, R., et al. 2014, *JGRA*, **119**, 1541